RSC Advances

PAPER

Cite this: *RSC Adv.*, 2019, **9**, 34299

Microstructural free volume and dynamics of cryoprotective DMSO–water mixtures at low DMSO concentration†

Katarína Čechová, [a] Igor Maťko, [a] Jaroslav Rusnák, [a] Helena Švajdlenková, [b] Ivan Klbik, [c] Ján Lakota *[def] and Ondrej Šauša *[a]

Received 13th August 2019
Accepted 17th October 2019

DOI: 10.1039/c9ra06305f

rsc.li/rsc-advances

This work investigates the free-volume properties of the dimethyl sulfoxide (DMSO)–water mixtures by positron annihilation lifetime spectroscopy over a wide temperature range of 20–320 K. The processes of melting and solidification of the water, DMSO and the DMSO–water mixtures at 1.8, 2.0 and 10% vol. DMSO respectively were studied. It was found that the recrystallization during heating of the water–DMSO cryoprotective mixtures above 160 K at low DMSO concentrations is affected by the amount of DMSO in the mixture. The amount of amorphous phase formed during cooling influences the hysteresis between cooling and heating cycles which could be crucial for cell survival. Experiments also show the time dependence of crystallization which indicates that rapid heating can suppress this secondary crystallization which is undesirable during the cell thawing process. Similar concentrations of DMSO (1.8% and 2% vol. DMSO in water) where a 2% vol. DMSO mixture secures cell survival but 1.8 vol% does not, showed differences in structural and dynamic properties that are key factors in cell survival. These results were supported by differential scanning calorimetry and low frequency dielectric spectroscopy measurements. The obtained data are in strong agreement with the observed cryoprotective efficacy of the DMSO–water mixtures on living cells.

Introduction

Biological and chemical processes in living cells slow down at low temperatures. Low temperatures allow long-term storage of cells and tissues. However, low temperatures and associated freezing are, for the most organisms, fatal due to the formation of intracellular and extracellular ice crystals which mechanically damage the cell and it causes cell death. Here the main problem is to overcome the phase transition of the conversion of liquid water into ice.[1]

The way to influence crystallization of water in the cell at low temperatures is by addition of a cryoprotective agent at a sufficient concentration without causing damage of the cell. The aim is therefore to find the lowest sufficient concentration of the cryoprotectant and to know its influence on the solidification and the melting processes in the mixture with water. The cryoprotective agent, in our case dimethyl sulfoxide, DMSO, affects the rate of water transport from the cell, nucleation and growth of ice crystals.[2] This substance shifts the phase transition of liquid water to ice towards lower temperatures and it also increases the portion of non-frozen liquid at low temperatures. It leads to the suppression of ice nucleation (crystalline phase) and promotes vitrification of water.[3]

The knowledge about freezing and melting of water is crucial for the successful cryopreservation of cells. Many processes are virtually mastered, but there are many unclear phenomena and obstacles that influence the efficiency of the cryopreservation of larger units such as organs. A deeper understanding of the cryoprotective mechanism of the DMSO–water mixture at the molecular level will allow to control and to set cryopreservation condition (*e.g.* cooling rate) increasing the viability of cells.

The studies with water are very well summarized in different works.[4] Properties of pure DMSO were examined by several techniques. Structural parameters of pure DMSO were investigated using neutron powder diffraction[5] and a recent study by a single-crystal X-ray diffraction technique at 100 K (ref. 6) showed a three-dimensional arrangement of DMSO molecules in the solid state due to the dominant C–H···O intermolecular interaction. There are works that modelled possible configurations of DMSO molecules into larger aggregates.[7,8]

[a]*Institute of Physics SAS, Dúbravská cesta 9, 845 11 Bratislava, Slovak Republic. E-mail: ondrej.sausa@savba.sk*

[b]*Polymer Institute SAS, Dúbravská cesta 9, 845 41 Bratislava, Slovak Republic*

[c]*Faculty of Mathematics, Physics and Informatics, Comenius University in Bratislava, Mlynská dolina F1, 842 48 Bratislava, Slovak Republic*

[d]*Biomedical Research Center SAS, Dúbravská cesta 9, 845 05 Bratislava, Slovak Republic. E-mail: jan.lakota@savba.sk*

[e]*St. Elizabeth Cancer Institute, Heydukova 10, 812 50 Bratislava, Slovak Republic*

[f]*Center of Experimental Medicine SAS, Dúbravská cesta 9, 841 04 Bratislava, Slovak Republic*

† Electronic supplementary information (ESI) available. See DOI: 10.1039/c9ra06305f

Substantially many articles refer to the properties of DMSO as the part of a mixture with water in more detail due to the importance of the topic investigating the physical properties of this cryoprotective mixture. Various methods and techniques have been used. The simulation of the molecular dynamics (MD) of the DMSO–water as an optimized structure has described the individual clusters that these molecules can generate. Based on modeling, the configurations of different types of clusters have been shown.[9–12] The expanded range of the glass transition of water was found *via* the molecular dynamics annealing simulations. This would correspond to the formation of a stronger glass in water–DMSO mixtures[13] and it brings some new insights into the mechanism of cryoprotection at the molecular level. MD simulations in combination with the infrared absorption spectroscopy for identification of the S=O stretching mode directly quantify DMSO–water hydrogen-bond populations.[14]

In the work,[15] changes in the thermal conductivity of the dimethyl sulfoxide (DMSO) solution between the crystalline and vitrified states as well as in thermal conductivity around eutectic temperature are shown. The freezing temperature curve in DMSO–water solutions was published earlier by R. N. Havemeyer.[16] The mass spectrometric study of DMSO–water binary mixture was done by D. N. Shin *et al.*[17]

Several papers dealt with the dynamic properties of mixtures from the viewpoint of dielectric studies,[18–22] using also a low frequency range for the area of static permeability.[23,24]

However, the most articles examine the properties of DMSO–water mixtures within a wide range of concentrations. The properties of mixtures with very low concentrations of DMSO are often overlooked and the data in the literature are mostly absent. Experimental studies are mainly related to the standard techniques mentioned above.

A very perspective experimental technique for the investigation of substance properties at the microstructural level *via* free-volume approach is positron annihilation lifetime spectroscopy (PALS).[25,26] PALS is a unique nuclear physics technique which monitors positron annihilation and measures the lifetime of positrons in a substance. In many substances, the bonded state of the electron and positron, so called positronium (Ps), is formed during the thermalization of the positrons after penetration into matter. The triplet state of Ps, *ortho*-positronium (*o*-Ps), is a suitable probe for the study of free volumes.[27] The measured lifetime of *o*-Ps allows to determine the average sizes of microstructural free volumes (defects, cavities, pores) in the range of 0.1–50 nm using suitable models. The uniqueness of the PALS technique lies in the ability to characterize local free volumes at the molecular level and their changes due to changing external conditions (*e.g.* temperature, pressure, time, *etc.*). Changes in free volumes with temperature (expansion or shrinkage) give important information about the freezing or melting of the materials, and give the opportunity to confront such experimental results with other techniques or computer simulations of molecular dynamics. PALS is relatively simple and non-destructive technique, which is another benefit.

The investigation of physical properties of DMSO–water system using the PALS technique strongly absents. The aqueous solutions with different concentrations of DMSO were examined at room temperature[28] and experimental results were interpreted in the framework of liquid pseudo clathrate structure. Previously it has been shown that DMSO at rather low concentrations (2% and 2.2% vol. respectively) can be cell protective during their cryopreservation.[29,30]

In the present work, the effect of different low concentrations of DMSO (1.8, 2.0 and 10% vol. respectively) on the solidification and melting of water through the changes in microstructural free volumes by the positron annihilation lifetime technique were investigated in the wide-temperature range from 20 K up to 320 K. Moreover, these results were supported by other experimental techniques such as differential scanning calorimetry (DSC) and low frequency dielectric spectroscopy (DS).

Experimental

Samples

The pure water LC-MS Ultra CHROMASOLV from Honeywell/Riedel-de Haen and dimethyl sulfoxide (DMSO, C_2H_6OS), anhydrous 99.9% from Sigma-Aldrich were used. Concentration of the DMSO in the water is here defined as the ratio of volumes $(V_{DMSO}/(V_{DMSO} + V_{water})) \times 100\%$.

The mixtures with a defined ratio of volumes of individual constituents were placed in sample containers for PALS, DSC and DS devices.

PALS

The time resolution of the fast–fast positron lifetime spectrometer was about 320 ps (FWHM). The standard sandwiched geometry of the source-sample assembly was used. ^{22}Na source covered by Kapton windows is placed between two identical sample chambers which are screwed down. Such prepared sample chamber is connected to cooling part of cryogenerator and fixed between two detectors of PALS spectrometer. The time resolution function was determined by Al defect-free sample. The correction to annihilation in the Kapton foils (8 μm) of the positron source as well as the window of the sample chambers was taken into account. The activity of positron source was about 1 MBq.

Temperature measurements in the range of 20–320 K were done by the closed cycle He-refrigerator JANIS CCS-450 System with stability of temperature about ±0.2 K. The hermetically closed sample containers were kept under vacuum during temperature experiments.

LT program[31] was used for the analysis of lifetime spectra. Three lifetime components were used during this analysis. The shortest lifetime is attributed to the *para*-positronium (*p*-Ps) annihilation that was fixed to the value 125 ps, medium component came from the positron annihilation without Ps creation and the longest lifetime (in nanosecond range) originates from the pick-off annihilation of *ortho*-positronium (*o*-Ps) in local free volumes of different sizes. The pick-off annihilation is the process, where the positron from *o*-Ps annihilate with an electron from the surface of pores and shorten *o*-Ps lifetime

depend on pore size. The ratio of *p*-Ps and *o*-Ps intensities was fixed to 1 : 3. The average free volume pore sizes in solid state were estimated from the *o*-Ps lifetimes ($\tau_{o\text{-Ps}}$) using well known semiempirical equation for the spherical-shaped cavity approximation:[32,33]

$$\tau_{o\text{-Ps}} = 0.5[1 - (R_h/(R_h + \Delta R)) + (2\pi)^{-1} \sin(2\pi R_h/(R_h + \Delta R))]^{-1}, \quad (1)$$

where R_h is radius of the spherical free volume cavity and $\Delta R = 0.1656$ nm is an empirical parameter. The average free volume of a cavity was calculated as

$$V_h = 4\pi R_h^3/3. \quad (2)$$

A special case of annihilation in liquids will be discussed in the PALS section.

Differential scanning calorimetry (DSC)

DSC measurements were performed using power-compensation DSC8500 (PerkinElmer) with automatic intracooler (200 K). Investigated samples were encapsulated in air into aluminium pans and measured in dynamic nitrogen atmosphere. The cooling and heating regimes with the rates of 2.0 K min^{-1} were performed. Each DSC measuring cycle started at 303.0 K and the cooling as well as heating procedures were used. Firstly, each sample was slowly cooled to 213.0 K, sufficiently below the equilibrium crystallization temperature of water, where the solidification was studied. Then the sample was continuously heated up to 303.0 K and the corresponding melt transition was detected.

Dielectric spectroscopy (DS)

The complex permitivity spectra were measured by an impedance analyser WK6500B, Wayne Kerr Electronics, in the range of frequency from 20 Hz to 100 kHz. The temperature measurements were performed in the simple cryostat cooled by liquid nitrogen. The measurements were performed in the heating cycle with the heating rate approximately 1.8 K min^{-1} between measurements. The block diagram of measurements at various temperatures with other details is in Fig. S1 of ESI.†

Results and discussion

PALS

The lifetime temperature dependencies of *o*-Ps for DMSO, water, and two-component mixtures of 1.8, 2 and 10% vol. DMSO in water were measured. Two measuring cycles, heating and cooling, were performed for each sample. Since the lifetime of *o*-Ps reflects local free volumes in the solid or the viscous supercooled liquid state, they are very sensitive to the phase or the dynamic transformations in the investigated substances. The shape of the temperature dependence $\tau_{o\text{-Ps}}(T)$ implies whether it is a crystalline or amorphous state. The time evolution of solidification or melting processes can be investigated as well.

We have to note that the relation (1) in the high temperature range, where $\tau_{o\text{-Ps}}$ with increasing temperature changes slowly and reaches liquid plateau region, gives slightly different values of intermolecular free volume sizes compared to other physical methods.[34] The bubble effect at the positronium formation[26,35,36] is one of the possible explanations for these differences in the liquid state with low viscosity. Ps creates a bubble in its surrounding and does not reflect the actual intermolecular space. For this reason, the V_h scale in the temperature dependences of *o*-Ps lifetimes in the liquid state does not represent the true size of the free volume but the Ps bubble size. In the supercooled region, vitreous and crystalline states, displayed V_h values are correct within the used model.

Pure DMSO

The comparisons of *ortho*-positronium lifetime, $\tau_{o\text{-Ps}}$ (or V_h calculated by eqn (1)) dependencies over a wide temperature range for the investigated compounds are shown in Fig. 1. At first sight, the different local free volume behavior of pure DMSO against other mixtures and pure water can be seen. In particular, there is a significant difference in the heating and the cooling cycles (expansion and contraction of microstructural free volume V_h) in DMSO, especially in the temperature range 165–200 K DMSO has greater free volumes compared to other solutions and pure water, mainly at temperatures above 200 K.

Cooling measuring cycle. The DMSO sample was cooled with the cooling rate of 2.4 K min^{-1} (given by the cryogenic technical capabilities) to defined temperature and then the lifetime spectrum was measured isothermally 2 hours. The steps between measurements were 20 K to prevent crystallization as much as possible (Fig. 1, DMSO, dashed line). The temperature dependence $V_h(T)$ gradually decreases with decreasing temperature which is typical for amorphous substances. The dynamic transition temperature from the supercooled liquid to the glassy state, $T_g^{DMSO,PALS} = (165 \pm 15)$ K for the given

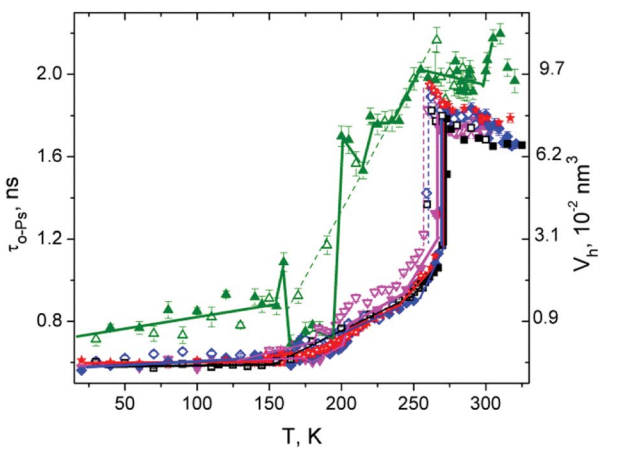

Fig. 1 *O*-Ps lifetime and calculated local free volume V_h temperature dependence for pure DMSO (▲), water (■), and the mixtures of DMSO in water (10% (▼), 2% (♦), 1.8% (*)). Measuring cycles: heating-full symbols, cooling-open symbols.

experimental conditions was determined from this curve. Below this temperature, V_h changed very little.

Heating measuring cycle. The sample was cooled "rapidly" from 300 K down to 30 K (cooling rate 2.4 K min^{-1}) and then stepwise heated with average heating rate of 0.15 K min^{-1} given by measuring time (2 h) at constant temperature and the next temperature step. There is minimal expansion of free volume up to 155 K. In this temperature region, the vitrified state generated by previous cooling can be considered. For this heating cycle, the estimated T_g for DMSO was 155 K which is in good agreement with value from literature.[37]

After heating of sample above 160 K, a significant jump contraction of V_h occurred indicating a structural transition. This could be, for example, phase transition–crystallization, as observed, for example, in propylene carbonate, salol or *m*-toluidine[38] where an amorphous form is heated above T_g. Such behavior of V_h is a consequence of a tightly arranged molecular structure and thus reduction of the intermolecular space. In the range 165–195 K, it is possible to ascribe the minimal local free volume values V_h to crystalline structure.[6]

In a further heating above 195 K, there was a significant step expansion of the V_h typical for the melting or rearrangement to a looser structure followed by a slow expansion of V_h with some fluctuations in the range from 200 K to the melting point (T_m). Such complicated sample behavior indicates that only a part of the sample was more tightly arranged (or crystallized) in the heating process and such structural arrangement is unstable above 195 K. Above 195 K, a tighter arrangement of the structure is only in certain parts – domains where some crystallization nuclei are present, and the rest remained amorphous (supercooled liquid). This is evidenced from the $V_h(T)$ dependence at higher temperatures where a typical "amorphous dependence" was obtained at cooling cycle with gradual (not sharp) changes of $V_h(T)$ observed also at another amorphous substances.[39] In addition, in heating cycle, the $V_h(T)$ fluctuations from "amorphous curve" occur in the temperature range of 200–240 K. These fluctuations could be associated with the reorganization of intermolecular distances due to rearrangement of molecular clusters of different types[8] in DMSO. Finally, the crystalline domains which did not melt above 195 K melt at $T_m = 291$ K, resulting in an increase in V_h. This is evidence that the crystalline phase was created in the DMSO sample in a some extent (amorphous curve is dominant) at these experimental conditions. Since melting at two different temperatures was observed, one could deduce from this the presence of two different crystalline phases.

The complex relative intensity $(I_{p\text{-Ps}} + I_{o\text{-Ps}}) = I_{Ps}$ of the time spectrum (see Fig. 2) attributes to amount of annihilation sites of Ps or creation probability of Ps in the substance DMSO. In the low temperature region, I_{Ps} showed sharp fluctuations in values with a peak of about 195 K and the following minimum at 205 K. Such behavior usually indicates phase transition or other changes in the structure of the material associated with rearrangement of the electron structure, where electrons are less available for the creation of Ps. In this case, the onset of the changes in the I_{Ps} during heating corresponds to the increase of $\tau_{o\text{-Ps}}$ (or V_h) connected with melting of the crystalline structure discussed above. A study of the crystalline arrangement of molecules in DMSO at

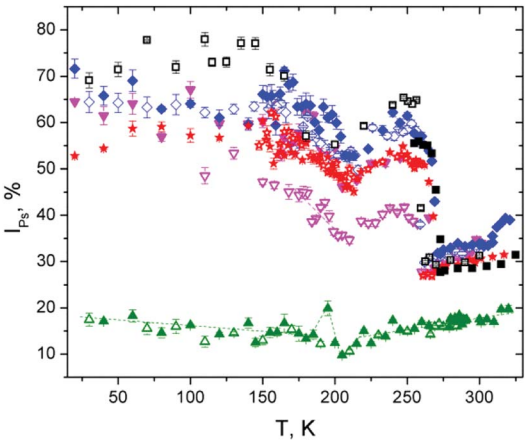

Fig. 2 Relative intensity I_{Ps} for the DMSO (▲), water (■), and their mixtures (10% (▼), 2% (♦), 1.8% (*)). Measuring cycles: heating-full symbols, cooling-open symbols.

100 K was done in the paper of Reuter.[6] Above this temperature, the intensity slowly increases without significant fluctuations. In the vicinity of T_m, the complex intensity of pure DMSO did not change with temperature in this experiment.

It can be seen from $\tau_{o\text{-Ps}}$ and I_{Ps} dependencies that the solidification and melting processes of DMSO are not simple, and they depend largely on the rate of cooling and heating as well as the temperature itself and, of course, the presence of potential crystallization nuclei that could initiate crystallization at least in the part of the sample volume. Local free-space behavior is complicated due to weak hydrogen bond interactions between molecules that change local electron density and result in tighter ordered structures, clusters of different sizes and configurations, as it was mentioned above. With gradual slow heating, the structure/cluster arrangement changes. Since the *o*-Ps probe is very sensitive to local electron density, it can sensitively indicate such changes.

Pure water

The temperature dependence of $\tau_{o\text{-Ps}}$ in water was measured precisely some time ago[40] and therefore this dependence is shown only for comparison to other investigated substances. When the temperature in the solidification process is lowered, water undergoes undercooling and there is a sharp drop in V_h implying the water crystallization. The real crystallization temperature depends on many factors, such as the presence of crystallization nuclei, but the temperature is not lower than the temperature limit of the homogeneous nucleation 231 K at the common laboratory conditions.[4] Thus a hysteresis curve is observed only in this region between the crystallization and melting temperatures. Below the crystallization temperature, we did not observe in our experiment any differences in *o*-Ps lifetime between heating and cooling cycles, similar to the other recent experiments.[40] The $V_h(T)$ dependence decreases linearly to 150 K and it is without change below this temperature. It is a case of slow cooling rates given by PALS experiment and not the case of extremely fast cooling where amorphous water or other forms of ice can be formed.

At low temperatures during heating, V_h is virtually unchanged and overlaps the cooling curve. V_h increases from the temperature of 150 K, then it follows a more intensive increase of V_h in a short temperature interval before T_m ("premelting" effect) and finally, V_h rapidly changes at T_m. An increase of the lifetime of *o*-Ps above 150 K is explained by the capture of *o*-Ps in temperature-created defects of the crystalline ice structure, mainly vacancies.[41,42]

We use the terminology "premelting effect" in this manuscript for the increase of $\tau_{o\text{-Ps}}$ below T_m associated with an additional increase of the vacancies size in ice. Another meaning of the term "premelting" according to study Zgardzińska *et al.*[43] relates to the local melting of the structure due to the accumulation of energy in the blob at the end of positron track in a very narrow temperature range (lower than 1 K) around T_m. This effect was not considered in this work.

Above T_m, $\tau_{o\text{-Ps}}$ decreases with an increase of temperature and it is consistent with literature data.[44] Such a precisely measured dependence in the range of 273–323 K has been explained, *e.g. via* the Ps-bubble model and existence of two states of water with different types of molecular bonds.[44] Another explanation of this phenomenon is through *o*-Ps reacting with spur reactants as hydroxyl radicals (OH), H_3O^+ cations and hydrated electrons.[45]

The temperature dependence of complex relative intensity I_{Ps} shows significant changes at melting (273 K), crystallization (around 264 K) as well as a local minimum at 210 K. As noted above for DMSO, the intensity of Ps formation is influenced by several factors, mainly by the concentration of local free volumes, but also by the chemical–physical influences that can suppress Ps formation.[27] Water ice is known for high Ps formation,[41] so that I_{Ps} increases considerably when water solidifies, as seen in Fig. 2. However, it is complicated to clearly interpret the decrease of I_{Ps} below 255 K. As indicated above, this decrease in I_{Ps} may be caused by a change in the concentration of local free volumes due to reorganization of intermolecular structure and the rearrangement of hydrogen bonds below 255 K. The existence of a greater number of strong tetrahedral hydrogen bonded water molecules[46] and water clusters[47] with their increased population with decreasing of the temperature has been described. In addition, the deviation from the extrapolated surface tension behavior was found below 235 K.[48] Such complex phenomena and reorganization of cluster structure can be responsible for the reduced Ps formation, and hence decrease I_{Ps}, at lowering of temperature from 255 K (or 235 K) to 210 K. This effect could be a subject for further study.

Water–DMSO mixtures

The two-component water–DMSO system, especially for low DMSO concentrations, is much more interesting from a biological point of view. Such mixtures still have strong cryoprotective effects on the cells at low temperatures with minimizing damage of cells by DMSO. The cryoprotective effect disappears quite suddenly in the system with a lower DMSO content, *i.e.* 1.8 vol% and lower.[30] Therefore, three DMSO/water mixtures consisting of 10%, 2% and 1.8% of DMSO were studied in relation the pure DMSO and water samples.

Fig. 3 shows the temperature dependencies of the $\tau_{o\text{-Ps}}$ and V_h of the mixtures, DMSO and water in the temperature range of 140–260 K. The figure shows the course of cooling and heating under specific experimental conditions (temperature step 3 K, isothermal measurement time 8100 s, positron source activity 2 MBq, polyimide (Kapton) window of sample chambers). An important finding for these mixtures is that the differences between $\tau_{o\text{-Ps}}$ (or $V_h(T)$) for cooling and heating cycles exhibit hysteresis. In addition, there is a rather substantial correlation between cryoprotective effects and the behavior of local free volume at low temperatures. The quantity measure of hysteresis behavior can be the area between the cooling and heating curves in the 140–260 K temperature range and it is proportional to the cryoprotective effect of these mixtures. In Table 1, the hysteresis area values of the $\tau_{o\text{-Ps}}(T)$, $I_{Ps}(T)$ curves for the volumetric concentrations DMSO in water of 1.8, 2, and 10% DMSO as well as the cell viability value (% of total survivors)[30] are shown. Lifetime $\tau_{o\text{-Ps}}$ is proportional to average size of the local free volume and its relative reduction at the different temperatures well indicates changes in the structure (*e.g.* dense packing at the crystallization).

For the sake of completeness, we also refer to the hysteresis areas for complex intensity I_{Ps} in Table 1. As mentioned above for pure substances, the interpretation of changes in I_{Ps} is more complicated than changes of $\tau_{o\text{-Ps}}$.[49] The overall nature of the temperature dependence of I_{Ps} is very similar to pure water, but the influence of DMSO is visible, which reduces Ps formation in the individual mixtures and at the same time causes hysteresis due to the amorphous phase present, indicated by the temperature dependence of $\tau_{o\text{-Ps}}$. The simplest explanation of hysteresis can be that the presence of the amorphous phase is characterized by a smaller number of larger cavities (I_{Ps} is proportional to concentration of local free volumes and $\tau_{o\text{-Ps}}$ to free volume size) and the number of local free volumes increases after recrystallization in the heating cycle which affects Ps creation. But there is still a possible chemical

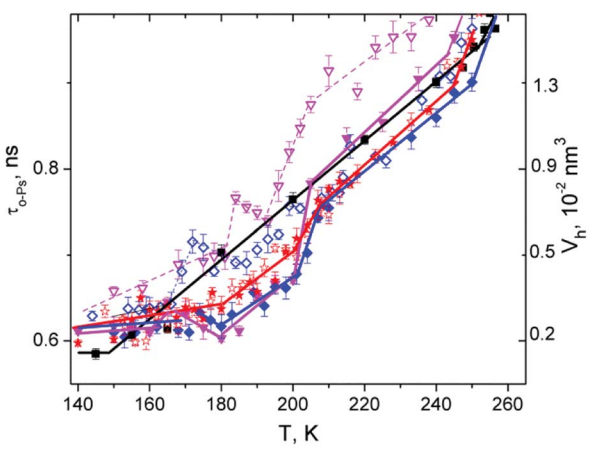

Fig. 3 Temperature dependence of $\tau_{o\text{-Ps}}$ and V_h for the selected vol. DMSO concentrations 10% (▼), 2% (♦), 1.8% (*) in water. Pure water (■) is as the reference. Heating cycles-full symbols, cooling cycles-open symbols (higher values and dashed lines). Lines are for the guide of eyes.

Table 1 Hysteresis area for temperature dependence of $\tau_{o\text{-Ps}}$, I_{ps} and cell viability for observed DMSO concentrations

Concentration of DMSO	1.8%	2%	10%
Difference area $\tau_{o\text{-Ps}}$, ns K	0.6	4.5	8.7
Difference area I_{Ps}, K	66	245	1074
Viability[30]	33	58	65

influence, associated with the formation and disintegration of molecular clusters of the mixtures, on Ps creation (expressed by I_{Ps}) in the cooling and heating cycles.

In Fig. 4, $\tau_{o\text{-Ps}}(T)$ dependence shows an example for the difference area between cooling and heating curves for a DMSO 10% mixture (cryoprotective standard).

In this experiment, the importance of the structural transitions in DMSO in the region of 165–200 K has been shown, and this effect is also transferred to the DMSO/water mixtures with varying degrees.

During the cooling of the investigated mixtures, the liquid is undercooled, followed by crystallization (ice creation accompanied by sharp decrease in $\tau_{o\text{-Ps}}$ or V_h, typical for the phase transition). However, a small fraction of amorphous structure remains in the sample during cooling, indicated by hysteresis behavior of the cooling–heating curve. The specificity of this system is represented by the influence of amorphous-like DMSO, which, when mixed with water at high DMSO content, has amorphous properties,[15] influences on the formation of local architecture of the molecules of the DMSO–water mixture, *via* creation of different cluster formation,[14] and ultimately on the behavior of the structure at low temperatures, especially in the region of 165–200 K, which has already been mentioned above. From the point of view of free-volume manifestations (hysteresis behavior), it can be concluded that a certain fraction of non-crystalline domains are generated in the volume at the cooling, which increases the effective V_h with increasing DMSO content (see max. values for V_h, cooling, 10% DMSO, Fig. 3). The reduction of V_h during cooling does not occur uniformly, but it falls below 205 K more sharply with a hint of more complex structure rearrangement (local free volume). At next cooling, it can be assumed that in a deep-frozen state below 155 K a substantial change in structure does not occur and the V_h is almost unchanged under 140 K.

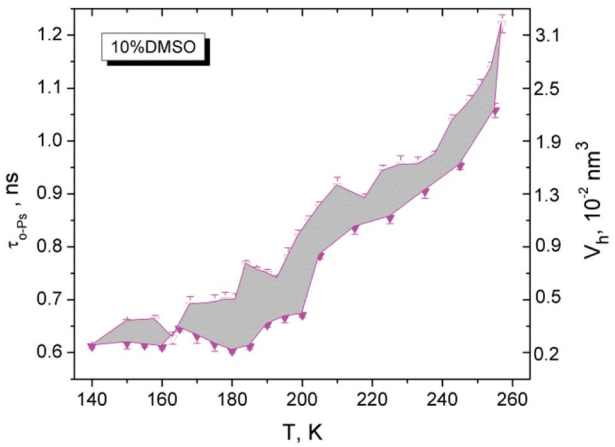

Fig. 4 Difference of $\tau_{o\text{-Ps}}$ values between cooling and heating cycles of 10% DMSO (open and full symbols, respectively).

During heating, the hysteresis behavior of V_h is observed, more markedly above 165 K. Here, the local free volume is more closely arranged, presumably with increasing the fraction of crystalline domains during heating and this more tight arrangement occurs in range 165–200 K. The amorphous fraction is reduced in this temperature range and the $V_h(T)$ has a lower V_h values than in the cooling cycle. The hysteresis area could be a measure of the disappearance of amorphous phase, which have the cryoprotective effect of the DMSO/water mixtures.[47] The maximal losses of amorphous phase appear in the temperature range of 165–200 K (Fig. 4).

Therefore it is important to overcome this "dangerous" temperature region by a fast heating that is crucial at the thawing of biological material. It prevents the tight structure, *i.e.* the formation of large ice crystals with fatal consequences on cell structures in the cryoprotective mixture. In Fig. 3, the mixture 10% DMSO has the biggest difference between the cooling and heating curves compare to the investigated mixtures, which means the largest fraction of the amorphous phase in the sample at the beginning of cooling. The mixture 2% DMSO still exhibits a rather pronounced hysteresis so that an amorphous phase still exhibits the sufficient cryoprotective effects.[47] A small change in the concentration of DMSO from 2% to 1.8% significantly changes the sample behaviour in which the hysteresis is greatly reduced as seen by a minimal difference between responses obtained from cooling and heating. The reduction of cryoprotective effect in 1.8% DMSO sample could be due to a minimal part of amorphous phase in the structure, which is not able enough to suppress the crystallization.

The effect of DMSO and its properties is evident in mixtures with water. In cooling regime, amount of DMSO influences formation of an amorphous fraction that suppresses crystalization. But recrystallization may occur by undercooling of the sample below T_g and next heating above this temperature, as was found in *m*-toluidine.[36] Holding the sample at a constant temperature in the range of 165–200 K for several hours results in the disappearance of the amorphous phase (recrystallization). The disruption of the part of complex structure during heating occurs at around 203–205 K.

The experiments shown some important facts for the studied mixtures as follows: the increase of V_h at temperature interval from 195 K to 205 K indicates a destruction of these more tightly arranged structures (melting). This process is associated with the presence of DMSO molecules. It was not observed in pure water. There is a certain limit of DMSO (1.8% vol. or 0.0047 mol. fraction) below which the hysteresis disappears, and the mixture resembles pure water.

The different degree of recrystallization and hence the hysteretic behavior of the mixtures can be explained by several factors. It is known that different DMSO-aqueous clusters are formed in the mixture,[14] which, above a certain concentration of DMSO, can form a more compact spatial network, the range of which depends on the amount of DMSO molecules in the

mixture. We suppose it can be a competing structure to crystalline ice domains. It is a question of further exploring the features and spatial arrangement of such competing entities (amorphous or/and crystalline). The presence of small domains with a DMSO local representation with a 0.35 molar fraction cannot be excluded. It is known that melting of a eutectic mixture with a molar fraction of 0.35 occurs at the melting point of about 203 K.[35] It is a question whether such a local arrangement of molecules and concentrations can be spontaneously created in small domains of aqueous mixtures.

Another contribution to recrystallization of partial volume may be the crystallization of interfacial water, which can be between the crystalline domains of ice and did not have enough time to crystallize in the first cooling cycle. However, this water does not explain the melting of the structure over 195 K. Our range of investigated concentrations is considerably low and represents substances with a larger amount of water and thus the small differences of T_m for water and the mixtures are detected.[16]

Fig. 5 documents the time dependence of $\tau_{o\text{-Ps}}$ at selected temperatures in the above-mentioned temperature range of 10% DMSO, which is a cryoprotective standard. We have to note that this time dependence was measured later than another sample and therefore the generated cooled structure is not completely identical to the presented substance in Fig. 3. Here, the lifetimes are shifted in the absolute scale. We can see in Fig. 5 that V_h at 160 K is stable for 3 h. Subsequent rapid heating to 180 K suggests the stable structure (quasi constant $\tau_{o\text{-Ps}}$ or V_h) during two hours, but the value is higher than at 160 K.

However, the V_h value drops sharply after 2 hours (nucleation process) and stabilizes in the next one-hour measurement. Closer rearrangement of the structure occurred in a part of the sample. Next, we can see a gradual increase of V_h up to a temperature of 205 K at defined conditions of the experiment (in the heating regime the step 2 K per two hour measurements at constant temperature), where V_h grows more slowly and follows the trend of water. Another point of interest is that in the region of 195–203 K, the first measured value of V_h has been systematically higher in comparison to the next one. It can be due to a change in dynamics of the structure causing an increase in local free volume and the relaxation of the structure. This phenomenon will inevitably be studied in future experiments.

The behavior of Ps formation in liquid mixtures is not easy.[27] In the temperature region above T_m, the formation of Ps in the liquid substances depends on the composition. By comparing I_{Ps} at room temperature 295 K *versus* DMSO concentration (Fig. 6), we received a non-linear dependence of I_{Ps} as a function of the amount of DMSO in mixture. It is a qualitatively similar relationship with the maximum for 2% DMSO sample as measured in the work.[28] Ps formation is probably strongly influenced by chemistry – it means different amounts and types of hydrogen bonds between molecules of the forming clusters in the mixtures. It can be stated that 1.8% DMSO is similar to water and 2% DMSO resembles the 10% DMSO cryoprotective standard.

DSC

DSC analysis of DMSO–water mixtures revealed several facts. Melting peaks of all three studied mixtures are comparable to pure water and pure DMSO using normalized scale (in Fig. 7). For lower content of DMSO in the mixtures, there is an evident effect of the peak broadening. The increasing of heat flow for pure water due to melting starts at the value of normalized temperature over 0.98. For 1.8% and 2% mixtures of DMSO, the increase of heat flow at value around 0.92 was observed. For the concentration 10% DMSO, the value of heat flow increases from point below 0.80, which is closer to the pure DMSO. The peak broadening is typical for melting of inhomogeneous and/or partially crystallized materials.[50] Similar broadening of DSC peaks were registered in the case of glycerol–water mixtures due to presence of different structural domains.[51]

From this point of view, the peak shape indicate that the mixture with 2% DMSO in comparison with 1.8% DMSO shows a higher degree of structural inhomogeneity due to the presence of other phases besides standard ice. It is caused by weaker bound sites of the clusters, *e.g.* interfacial water supposed by Y. Hayashi *et al.*[51]

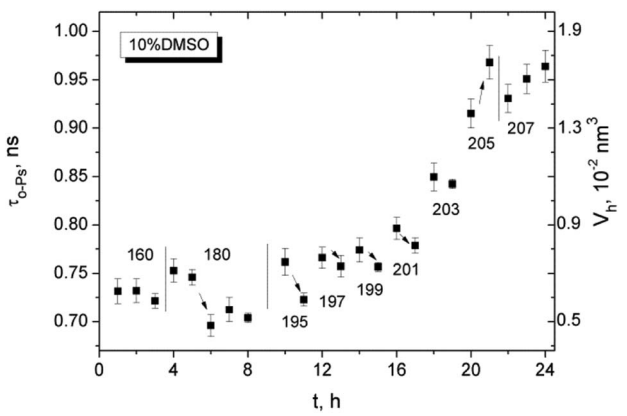

Fig. 5 Time evolution of $\tau_{o\text{-Ps}}$ or V_h at 160 K, 180 K and next in heating within the temperature interval of 195–213 K for the cryoprotective standard 10% DMSO in water. The numbers are the temperatures in Kelvin.

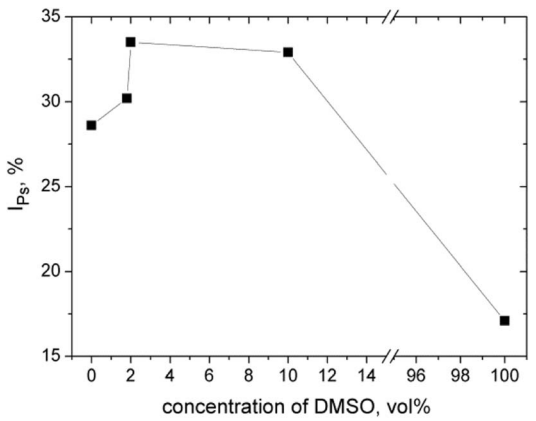

Fig. 6 Positronium creation in the mixtures DMSO–water in liquid state at 295 K. Intensity I_{Ps} *versus* volumetric concentration of DMSO in water.

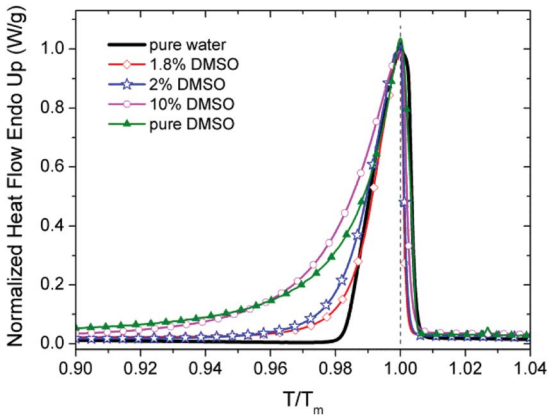

Fig. 7 Normalized heat flow for DMSO, water and mixtures of DMSO in water (1.8%, 2% and 10%). Heating cycles. Temperature scale normalized to the T_m (maximum of peak).

DS

Dielectric spectroscopy is a standard tool for monitoring the dynamics of low molecular weight systems. The response at different temperatures and frequencies and alternating electrical pulses may reveal important dynamic changes occurring in the sample such as various structural and phase transformations.[52,53] In our case, we used a simple approach for characterization of sample dynamic properties in the range of frequencies from 20 Hz up to 100 kHz. Although important relaxation peaks for water and DMSO are found at the higher frequency than 1 GHz,[21] but also lower frequencies in the static permittivity range[23,24] can also be used for the comparison of differences in dielectric properties of binary DMSO–water systems. It has been shown that water in the low-frequency range has a relative permittivity ε' dependent not only on temperature (ε' is nearly 80 at 20 °C as a widely accepted value[54]) but also on frequency.[55]

Dielectric spectra, the real (ε'), imaginary (ε'') part and their ratio tan $\delta = \varepsilon''/\varepsilon'$, for the cryoprotective standard 10% DMSO and for temperatures over 140 K are shown in Fig. 8. It can be seen the difference between liquid and solid phase and presence of relaxation phenomena. The increase of real part of the permittivity at low frequencies similar to another work[23] was explained as a result of polarization effects near surface of measuring cell due to ionic impurities in the investigated system.[23] In addition in solid phase, the relaxation maxima for ε'' are visible at low temperatures.

For better visibility of dynamic manifestations of 10% DMSO in the temperature scale, the temperature dependence of ε' and ε'' at the frequency of 70 kHz was used, in the area of static permittivity. At lower frequencies, the effect of dc-conductivity is strongly manifested and possible relaxation effects are less visible (Fig. 9a). The distinctive relaxation peak with a maximum of about 160 K (at 70 kHz) and changes indicating the melting of the crystalline structure can be seen.

A similar step-like or peak dependence for ε' and ε'', respectively, in the region near 200 K was measured for diethyl sulfoxide (DESO)–water system[56] with molar fraction $x_{DESO} =$

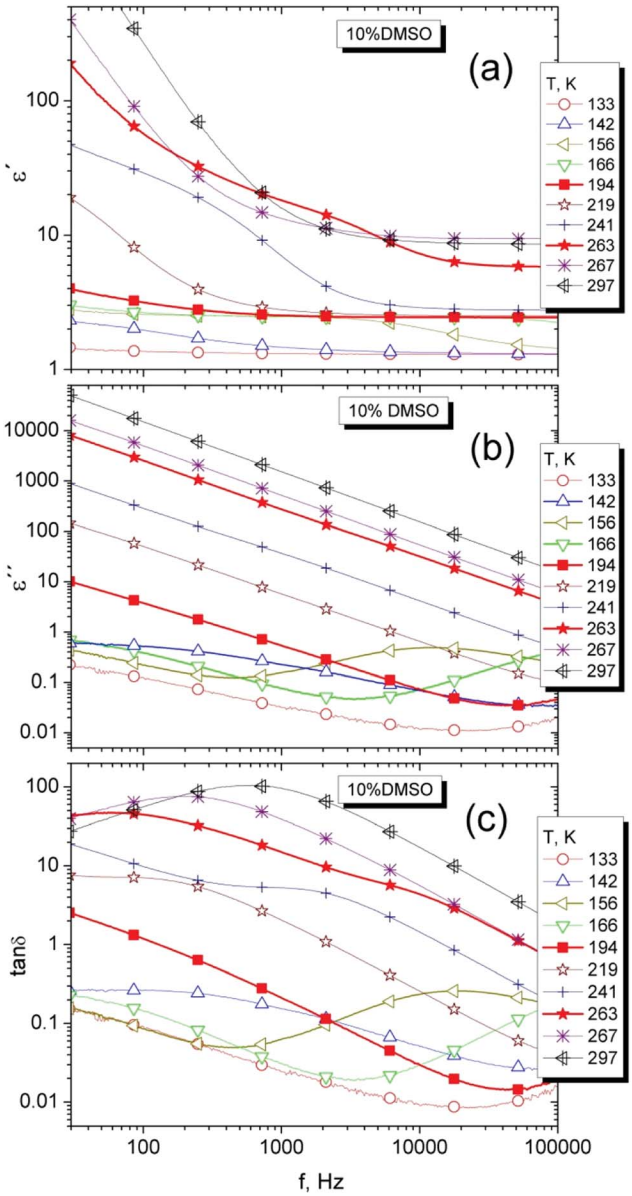

Fig. 8 Dielectric spectra, the real (a), imaginary (b) parts and the loss factor tan δ (c) of 10% DMSO mixture for selected temperatures.

0.3. Only one relaxation peak was observed at the absence of other relaxation manifestations associated with crystallization. At such "high" concentrations, DESO is a strongly glass-forming system and the peak was associated with relaxation of the amorphous structure.[56]

Fig. 9b shows the temperature dependence of ε'' for all samples investigated at a frequency of 70 kHz. A relaxation peak around 170 K is present only for strongly glass-forming DMSO and DMSO–water mixtures. This peak was not observed in the ice. Therefore this peak can be attributed to the dynamics of the amorphous phase in the substance.

In addition, the amount of the amorphous phase in the system can be qualitatively estimated from the magnitude of the effect for DMSO–water mixtures. The increased DMSO

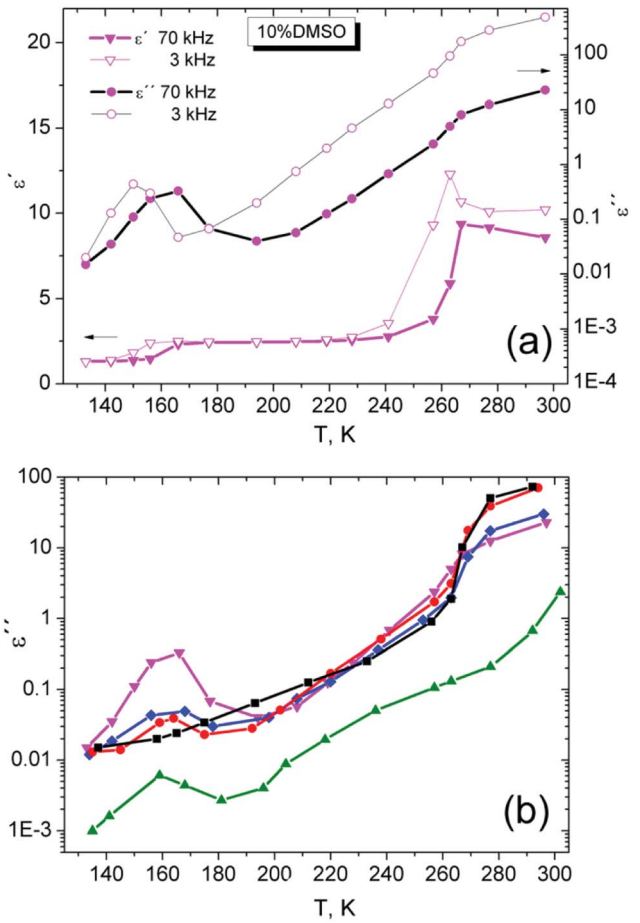

Fig. 9 Temperature dependence of real part ε' and imaginary part ε'' of the complex dielectric permitivity at the frequency of 70 kHz and 3 kHz for 10% DMSO mixture (a). Temperature dependence of ε'' at fixed frequency 70 kHz for pure DMSO (▲), water (■), and their mixtures (10% (▼), 2% (♦), 1.8% (★)) in the range from 140 K up to 300 K (b).

concentration in the mixtures increases the magnitude of the relaxation peak in a series of DMSO mixtures. This relaxation can reflect the presence of stronger intermolecular interactions of DMSO–water in comparison with DMSO–DMSO interactions which affect the properties and size of amorphous domains (amorphous phase) in the substance. For 1.8% DMSO, the suppression of such relaxation is obvious and figure shows very similar behavior ε'' compared to water around the melting point of the crystalline phase.

The dielectric response of the structure in the 165–200 K region, where PALS found differences in the hysteresis behavior of the samples, and just below the melting point were investigated. However, there is a strong contribution from dc-conductivity in this temperature and frequency range (see Fig. 8a and b). To highlight the changes in the dielectric spectra, the relative changes in dielectric losses were shown by the frequency dependence of tan δ for the investigated substances (Fig. 8c). This approach is non-standard in the DS due to a partial loss of information in such a representation. However, tan δ well characterizes the mutual changes between the real and imaginary part of the complex dielectric permittivity that can be used for qualitative comparison of samples.

Another reason of tan δ plot is to monitor the qualitative changes in the structure of the investigated substances, *i.e.* the presence of other relaxations associated with the non-amorphous phase mentioned above and reflected a background from dc-conductivity. Such multi-phase relaxation was found in the glycerol–water system (water rich mixtures) where the multiple sigmoids in the DS spectra $\varepsilon'(f)$ were observed.[51]

Fig. 10 shows the frequency dependence of tan δ for individual investigated substances. Only some temperatures are shown for clarity. The bold line shows the temperature areas where the amount of the crystalline phase should no change according to PALS experiments. The region starts above 200 K and ends at the melting of the crystalline phase. A distinct peak of tan δ can be seen in ice water as a typical crystallization system. This peak is separated by a wide "valley" from the slope at low frequencies from dc-conductivity, particularly observable at temperatures below the melting point. A similar "valley" is also seen at 1.8% and 2% vol. DMSO. However, the sample with 2% DMSO has this transition region reduced and 10% DMSO has this region strongly suppressed. For the sake of completeness, we report both $\varepsilon'(f)$ and $\varepsilon''(f)$ for the other investigated materials in ESI (Fig. S2†), except for the 10% DMSO shown in Fig. 8. It can be stated that the relaxations recorded in this region of frequencies and temperatures are due to the presence of a crystalline phase (ice).

It should be noted that in the region of the melting of crystalline phase (premelting) there is no shift of the peak with increasing temperature to higher frequencies.

The comparable steep transition of 1.8% of DMSO and water can be attributed to the melting of crystals. However, less steep trend of the melting effect in 2% and mainly in 10% DMSO suggests the reduced crystalline fraction and more amorphous character of the sample which can play the important role for cell survival.

Confirming the importance of clusters for the properties of DMSO–water mixtures could also be observed during the melting of sample at different heating rates. It is assumed that the melting of the crystalline phase in the water should occur in the entire volume at the same time and the melting temperature T_m is not dependent on the heating rate. If the melting depends on heating rate, it indicates the presence of other phase than crystalline one. The details about the measurements and the temperature dependencies of the imaginary part of the complex relative permittivity ε'' *versus* the heating rate for 10% DMSO as a cryoprotective standard are shown in ESI (Fig. S3†). The estimated average activation energy E_a of the process under investigation was 26.4 kJ mol^{-1}. It is close to the hydrogen bond energy 23 kJ mol^{-1} for the water,[57] we believe that this is a gradual breakdown of the clusters of DMSO–water network on the boundary of crystalline ice domains by breaking the hydrogen bonds in the melting process. PALS and DSC experiments with significant premelting effects also support this idea. Dielectric experiments showed directly the decomposition of hydrogen bonds in "premelting" of 10% DMSO and their important role for structure of studied compounds as well as presence of different phases at low temperatures. Such a complex structure of the hydrogen bond network in the water–

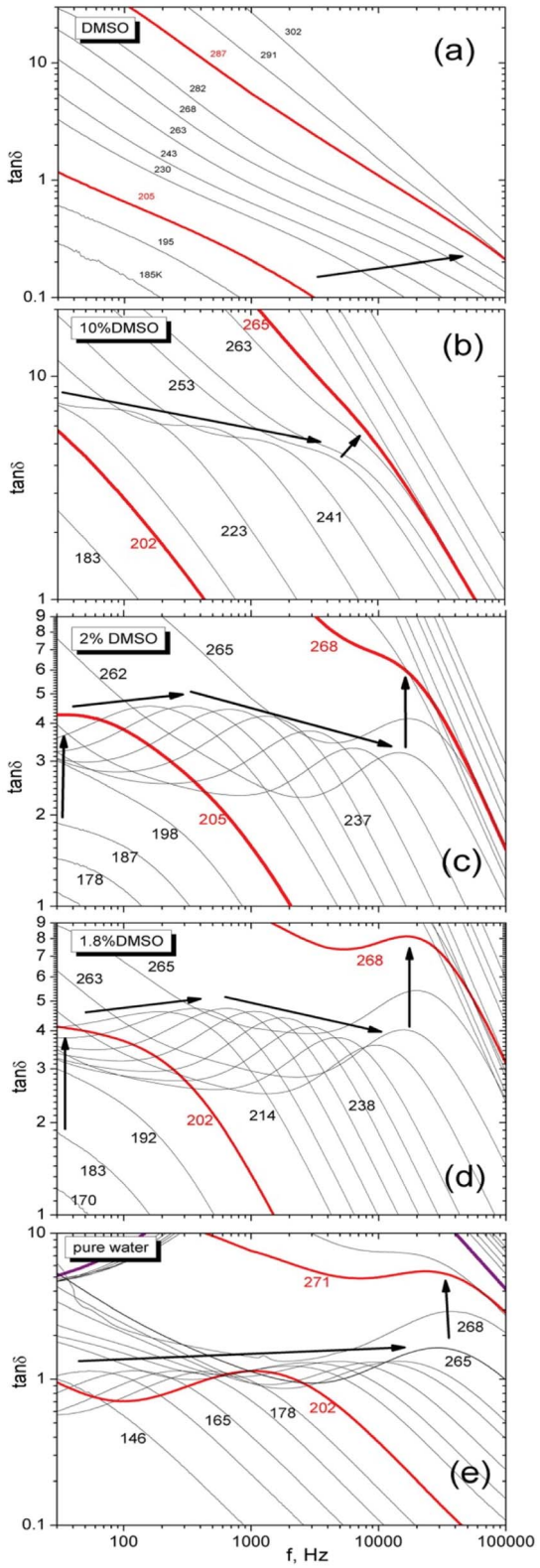

Fig. 10 The frequency dependence of tan δ at different temperatures for DMSO (a), 10% (b), 2% (c), 1.8% (d) and pure water (e). The coarse lines designate around melting temperature of the structures measured by PALS and the temperature near below T_m of the mixture, respectively. Arrows indicate tan δ peak movement with the temperature. Numbers mean the temperatures in K for better orientation. For clarity, not all temperatures are shown in figure.

DMSO[58] binary system is responsible for the physical properties of the investigated mixtures and hence ultimately for their cryoprotective effects (see also Fig. S4 in ESI†).

In many respects, the above facts are more or less a demonstration of the dielectric properties of the investigated substances and these facts classify 1.8% DMSO in their manifestations close to water and 2% DMSO more comparable to 10% DMSO cryoprotective standard, even with a small difference in DMSO concentration. This is due to differences in the molecular structure of the studied compounds, which form a complex system. A more detailed and deep study of the causes of such manifestations is essential in the future.

Conclusions

The dependence of *o*-Ps lifetime on the temperature during the heating and cooling cycles for dimethylsulfoxide, water and their selected mixtures were measured by the positron annihilation lifetime spectroscopy. The local free volumes reflect the melting and solidification processes of investigated substances in amorphous or crystalline state, respectively.

PALS revealed hysteresis behavior of $\tau_{o\text{-Ps}}(T)$ dependency (or $V_h(T)$) for cooling and heating cycles of selected DMSO–water mixtures and the hysteresis area is proportional to the cryoprotective effect. The hysteresis can be influenced by the amount of DMSO in the mixture where the concentration 2 vol% DMSO still has efficient cryopreservation effect.

The hysteresis behavior of the sample is influenced by the amount of DMSO in the mixture measured *via* the structural changes of the substance especially in heating. There is a closer arrangement of molecules in the 165–200 K range, in which additional crystallization occured in a amorphous part of the volume during rapid cooling. In other words, the concentrations of DMSO from 2% up to 10% in the mixtures create the amorphous phase in a sufficient amount during cooling providing the cryoprotective effects. In the case of the concentration of 1.8% DMSO, the mixture has only very few amorphous domains formed by cooling and this is not enough to suppress the growth of large ice crystals that are dangerous for cell structures.

The amount of a recrystallized phase can be reduced by heating rapidly over a critical temperature range of 165–200 K, where the structure rearrangement process needs the time, *e.g.* at 180 K the minimum of $\tau_{o\text{-Ps}}$ was reached after three hours. Fast heating minimizes disappearance of the amorphous phase generated during rapid cooling which suppresses the creation of large crystals of ice.

This temperature region of 165–200 K represents the dynamic instability of the structure indicating by the isothermal measurements of $\tau_{o\text{-Ps}}$.

DSC determined the melting behavior of the mixtures in which the "premelting" processes start earlier with increasing DMSO concentration. It suggests the presence of the higher structural heterogeneity, *i.e.* the presence of different types of structures competing with hexagonal ice, such as different types of molecular clusters.

Precise interpretation of the dielectric spectra of DMSO and water as well as their mixtures is complicated due to presence of different structural phases based on different combinations of hydrogen bonds between molecules. This is manifested by the presence of relaxation peaks in the DS spectra.

Dynamic study of a series of the mixtures at different temperatures exhibited that the amorphous and crystalline phases in investigated sample depend on DMSO concentration and revealed similar dynamic behaviour of samples with concentration of 2% and 10% vol. DMSO. On the other hand, 1.8% DMSO tends to water in its dynamic behaviour in the temperature range used mainly in temperature region near melting.

Simple DS experiments in this work do not claim a comprehensive answer but serve to support the conclusions of some PALS responses. Nevertheless, they suggest the requirement for more extended dynamic experiments by broadband DS in future.

In conclusion, despite the small volumetric concentration difference (1.8% and 2% vol.) of the mixtures, the physical properties of these mixtures studied by PALS, DSC and DS techniques were quite different. The main cause seems to be a complicated and extensive network of hydrogen bonds between the molecules, which influences the free-volume and dynamic properties of the mixtures depending on the composition and system temperature.

Although many of the facts summarized here give a possible explanation for the different behaviors of the studied mixtures with an impact on the cryoprotective properties, they also show the need of further investigation of the phenomena associated with narrow volumetric concentration range of DMSO near 2%. This approach of the study *via* local free volume showed that PALS, in combination with other techniques, is useful for monitoring the processes of solidification and heating of cryoprotective compositions. This technique introduces new perspectives on cryopreservation and allows to explain many empirical findings obtained in the study of the effects of cryoprotective compositions on biological structures.

Conflicts of interest

The authors declare no conflicts of interest.

Acknowledgements

This study was supported by the Slovak Grant Agency VEGA (projects no. 2/0157/17 and 2/0024/17), Slovak Research and Development Agency (projects no. APVV-16-0369 and APVV-0854-12) and the Foundation for Cell Transplantation. The authors thank Prof. Peter Lunkenheimer (University of Augsburg, Germany) for helpful comments.

Notes and references

1 T. H. Jang, S. C. Park, J. H. Yang and J. Y. Kim, *Integrative Medicine Research*, 2017, **6**, 12.
2 J. M. Karlsson, E. G. Cravalho and M. Toner, *J. Appl. Phys.*, 1994, **75**, 4442.
3 W. F. Rail and G. M. Fahy, 1985, **313**, 573.
4 http://www1.lsbu.ac.uk/water/supercooled_water.html.
5 R. M. Ibberson, *Acta Crystallogr.*, 2005, **61**, 571.
6 H. Reuter, *Acta Crystallogr.*, 2017, **73**, 1405.
7 Yu. I. Khurgin and A. N. Isaev, *Russ. Chem. Bull.*, 1992, **41**, 1046.
8 N. S. Venkataramanan and A. Suvitha, *J. Mol. Graphics Modell.*, 2018, **81**, 50.
9 B. Kirchner and M. Reiher, *J. Am. Chem. Soc.*, 2002, **124**, 6206.
10 B. Kirchner and J. Hutter, *Chem. Phys. Lett.*, 2002, **364**, 497.
11 S. Roy, S. Banerjee, N. Biyani, B. Jana and B. Bagchi, *J. Phys. Chem. B*, 2011, **115**, 685.
12 A. Idrissi, B. A. Marekha, M. Barj, F. A. Miannay, T. Takamuku, V. Raptis, J. Samois and P. Jedlovszky, *J. Chem. Phys.*, 2017, **146**, 234507.
13 J. B. Mandumpal, C. A. Kreck and R. L. Mancera, *Phys. Chem. Chem. Phys.*, 2010, **13**, 3839.
14 K. I. Oh, K. Rajesh, J. F. Stanton and C. R. Baiz, *Angew. Chem.*, 2017, **56**, 11375.
15 L. E. Ehrlich, J. S. G. Feig, S. N. Schiffres, J. A. Malen and Y. Rabin, *PLoS One*, 2015, **10**, 1.
16 R. N. Havemeyer, *J. Pharm. Sci.*, 1966, **55**, 851.
17 D. N. Shin, J. W. Wijnen, J. B. F. N. Engberts and A. Wakisaka, *J. Phys. Chem. B*, 2001, **105**, 6759.
18 S. M. Puranik, A. C. Kumbarkhane and S. C. Mehrotra, *J. Chem. Soc., Faraday Trans.*, 1992, **88**, 433.
19 Z. Lu, E. Manias, D. D. Macdonald and M. Lanagan, *J. Phys. Chem. A*, 2009, **113**, 12207.
20 L. J. Yang, X. Q. Yang, K. M. Huang, G. Z. Jia and H. Shang, *Int. J. Mol. Sci.*, 2009, **10**, 1261.
21 S. S. N. Murthy, *J. Phys. Chem. B*, 1997, **101**, 6043.
22 U. Kaatze, *Int. J. Thermophys.*, 2014, **35**, 2071.
23 I. Płowaś, J. Świergiel and J. Jadżyn, *J. Chem. Eng. Data*, 2013, **58**, 1741.
24 Y. Uosaki, S. Kitaura and T. Moriyoshi, *J. Chem. Eng. Data*, 1997, **42**, 580.
25 *Positrons Solid-State Physics*, ed. W. Brandt and A. Dupasquier, North-Holland, Amsterdam, 1983.
26 T. Goworek, *Annales Universitatis Mariae Curie-Sklodowska*, 2014, **69**, 1.
27 O. E. Mogensen, *Positron Annihilation in Chemistry*, Springer-Verlag, Berlin Heidelberg, 1995.
28 K. Jerie, A. Baranowski, B. Rozenfeld, B. J. Trzebiatowska and J. Gliński, *Acta Phys. Pol., A*, 1991, **79**, 507.
29 https://www.ncbi.nlm.nih.gov/pubmed/24964911.
30 J. Lakota and P. Fuchsberger, *Bone Marrow Transplant.*, 1996, **18**, 262.
31 J. Kansy, *Nucl. Instrum. Methods Phys. Res.*, 1996, **374**, 235.
32 S. J. Tao, *J. Chem. Phys.*, 1972, **56**, 5499.
33 M. Eldrup, D. Lightbody and J. N. Sherwood, *Chem. Phys.*, 1981, **63**, 51.
34 G. Consolati and F. Quasso, Morphology of free-volume holes in amorphous polymers by means of positron

annihilation lifetime spectroscopy, in *Polymer physics: from suspensions to nanocomposites and beyond*, ed. L. A. Utracki and A. M. Jamieson, Wiley, Hoboken, NJ, 2010.
35 R. A. Ferrell, *Phys. Rev.*, 1957, **108**, 167.
36 B. Zgardzińska, *Mater. Sci. Forum*, 2013, **733**, 29.
37 D. H. Rasmussen and A. P. Mackenzie, *Nature*, 1968, **220**, 1315.
38 V. Majerník, J. Krištiak, O. Šauša and M. Iskrová-Miklošovičová, *Mater. Sci. Forum*, 2013, **733**, 84.
39 O. Šauša, J. Zrubcová, P. Bandžuch, J. Krištiak and J. Bartoš, *Radiat. Phys. Chem.*, 2000, **58**, 479.
40 O. Šauša, M. Iskrová, B. Sláviková, V. Majerník and J. Krištiak, *Mater. Sci. Forum*, 2011, **666**, 115.
41 M. Eldrup, O. E. Mogensen and G. Trumpy, *J. Chem. Phys.*, 1972, **57**, 495.
42 O. E. Mogensen and M. Eldrup, *J. Glaciol.*, 1978, **21**, 85.
43 B. Zgardzińska and T. Goworek, *Phys. Lett. A*, 2014, **378**, 915.
44 K. Kotera, T. Sito and T. Yamanaka, *Phys. Lett. A*, 2005, **345**, 184.
45 S. V. Stepanov, V. M. Byakov and T. Hirade, *Radiat. Phys. Chem.*, 2007, **76**, 90.
46 F. Lehmkühler, Y. Forov, T. Büning, C. J. Sahle, I. Steinke, K. Julius, T. Buslaps, M. Tolan, M. Hakala and C. Sternemann, *Phys. Chem. Chem. Phys.*, 2016, **18**, 6925.
47 H. Kanno, A. Ohnishi, K. Tomikawa and Y. Yoshimura, *J. Raman Spectrosc.*, 1999, **30**, 705.
48 T. R. Rogers, K.-Y. Leong and F. Wang, *Sci. Rep.*, 2016, **6**, 33284.
49 O. E. Mogensen, *J. Phys. IV*, 1993, **3**, 1.
50 *Principles and Applications of Thermal Analysis*, ed. P. Gabbott, Blackwell Publishing, 2007.
51 Y. Hayashi, A. Puzenko, I. Balin, Y. E. Ryabov and Y. Feldman, *J. Phys. Chem. B*, 2005, **109**, 9174.
52 *Broadband Dielectric Spectroscopy*, ed. F. Kremer and A. Schönhals, Springer, Berlin, 2002.
53 P. Lunkenheimer, M. Köhler, S. Kastner, and A. Loidl, in *Structural Glasses and Supercooled Liquids*, ed. P. G. Wolynes and V. Lubchenko, Wiley, Hoboken, 2012.
54 B. Bagchi, *Chem. Rev.*, 2005, **105**, 3197.
55 A. Angulo-Sherman and H. Mercado-Uribe, *Chem. Phys. Lett.*, 2011, **503**, 327.
56 L. Gabrielyan, S. Markarian, P. Lunkenheimer and A. Loidl, *Eur. Phys. J. Plus*, 2014, **129**, 245.
57 S. J. Suresh and V. M. Naik, *J. Chem. Phys.*, 2000, **113**, 9727.
58 R. L. Mancera, M. Chalaris and J. Samios, *J. Mol. Liq.*, 2004, **110**, 147.